Acta Crystallographica Section D
Biological Crystallography
ISSN 0907-4449

Rotational order–disorder structure of fluorescent protein FP480

Sergei Pletnev,[a]* Kateryna S. Morozova,[b] Vladislav V. Verkhusha[b] and Zbigniew Dauter[c]*

[a]SAIC-Frederick Inc., Basic Research Program, Argonne National Laboratory, 9700 South Cass Avenue, Argonne, IL 60439, USA, [b]Department of Anatomy and Structural Biology, Albert Einstein College of Medicine, 1300 Morris Park Avenue, Bronx, New York 10461, USA, and [c]Synchrotron Radiation Research Section, MCL, National Cancer Institute, Argonne National Laboratory, 9700 South Cass Avenue, Argonne, IL 60439, USA

Correspondence e-mail: svp@ncifcrf.gov, dauter@anl.gov

Received 17 April 2009
Accepted 2 June 2009

PDB References: FP480, acidic form, 3h1o, r3h1osf; neutral form, 3h1r, r3h1rsf.

In the last decade, advances in instrumentation and software development have made crystallography a powerful tool in structural biology. Using this method, structural information can now be acquired from pathological crystals that would have been abandoned in earlier times. In this paper, the order–disorder (OD) structure of fluorescent protein FP480 is discussed. The structure is composed of tetramers with 222 symmetry incorporated into the lattice in two different ways, namely rotated 90° with respect to each other around the crystal *c* axis, with tetramer axes coincident with crystallographic twofold axes. The random distribution of alternatively oriented tetramers in the crystal creates a rotational OD structure with statistically averaged *I*422 symmetry, although the presence of very weak and diffuse additional reflections suggests that the randomness is only approximate.

1. Introduction

Steady progress in macromolecular crystallography and the availability of sophisticated and powerful algorithms and programs have made it possible to tackle crystal structures that display unusual or 'pathological' diffraction phenomena. Whereas more than a decade ago it was hardly possible to adequately refine protein crystal structures from merohedrally or pseudomerohedrally twinned crystals, today several programs can be used for this purpose [*SHELXL* (Sheldrick, 2008), *CNS* (Brünger *et al.*, 1998), *PHENIX* (Adams *et al.*, 2002), *REFMAC* (Murshudov *et al.*, 1997)]. In fact, merohedrally twinned cases in the Protein Data Bank (PDB; Berman *et al.*, 2000) are not infrequent (Lebedev *et al.*, 2006). Epitaxially twinned crystals display diffraction patterns in which more than one lattice is present and some reflection profiles overlap on the exposed rotation images. Examples of successful utilization of such crystals include antibody 17/9 (Schulze-Gahmen *et al.*, 1993), RNA dodecamer (Lietzke *et al.*, 1996), Lon domain (Dauter *et al.*, 2005) and an Fab–peptide complex (Dhillon *et al.*, 2008).

More complicated cases of crystal-growth irregularity are order–disorder structures or OD structures (Dornberger-Schiff, 1956; Dornberger-Schiff & Grell-Niemann, 1961), alternatively termed crystals with lattice-translocation defects (LTD; Wang, Kamtekar *et al.*, 2005; Wang, Rho *et al.*, 2005), in which successive layers of molecules in the crystal are shifted in alternative directions while preserving equivalent mutual contacts. Depending on the extent of the (ir)regularity of such shifts in the whole crystal, some classes of reflections in the corresponding diffraction patterns display a tendency to show modulated intensities and linearly diffuse profiles. Such a pathology, which is more often observed for small-molecule crystals, has also been described several times for crystals of

proteins. Bragg & Howells (1954) reported the characteristic abnormalities in the diffraction pattern of imidazole methaemoglobin crystals and provided a physical interpretation of this effect in terms of shifts in consecutive layers of molecules. A more rigorous mathematical interpretation of this phenomenon was provided by Cochran & Howells (1954). According to their theory, it may be possible to utilize the measured reflection intensities from OD crystals after applying appropriate corrections. This approach has been shown to lead to successful structure solution and refinement from OD crystals of proteins, as described in several studies. Trame & McKay (2001) described the *P*622 structure of *Haemophilus influenzae* HslU chaperone, in which the consecutive *a*,*b* layers consisting of hexamers are shifted by $\Delta x = 0.22$ along the *a* axis, causing a specific modulation of the intensities of reflections with odd *l* indices. Wang *et al.* (2005) reported the crystal structure and procedures leading to successful structure solution of φ29 DNA polymerase, which displayed alternating sharp and diffuse reflection profiles in consecutive layers with increasing index *l*. Rye *et al.* (2007) solved the structure of bacterial L-2-haloacid dehalogenase, consisting of stacked *a*,*b* layers of molecules mutually shifted by a fraction of the unit cell in the positive or negative *a* direction, which resulted in specific modulation of reflection intensities. The OD phenomenon has also been observed in crystals of horse erythrocyte catalase (Glauser & Rossmann, 1966), spinach RuBisCO (Pickersgill, 1987), SARS S1–antibody complex (Hwang *et al.*, 2006), H1N1 neuraminidase (Zhu *et al.*, 2008) and bacterial carboxysome shell (Tanaka *et al.*, 2008).

In our investigations of various fluorescent proteins, we obtained two crystal forms of the protein FP480 grown in solutions with different pH values. Both crystal forms are tetragonal *I*-centered. One of them was obtained under acidic conditions and has unit-cell parameters $a = 98.21$, $c = 108.06$ Å; the second, obtained from neutral solution, has parameters $a = 91.40$, $c = 53.53$ Å. Although their unit-cell parameters seem to be related, the data of the first form only merge in space group *I*4, while the intensities from the second crystal merge almost equally well in the *I*4 and *I*422 symmetries. However, the volume of the unit cell precludes the possibility of accommodating the 28 kDa molecule in the asymmetric unit of the *I*422 space group in the smaller cell. Moreover, close inspection of the diffraction images revealed very faint and diffuse reflections between the zones of consecutive *l* indices, suggesting certain abnormalities in the crystal structure of the smaller cell form of FP480. The structure of the larger cell acidic form has been successfully solved in *I*4 symmetry and its description and discussion will be published elsewhere. Here, we present the solution and interpretation of the crystal structure of the smaller cell neutral pH form of FP480.

2. Materials and methods

Prior to crystallization, FP480 was repurified by size-exclusion chromatography on a Superdex 200 column (GE Healthcare) in 20 m*M* Tris–HCl pH 8.0, 200 m*M* NaCl, 5 m*M* EDTA. Buffer exchange and protein concentration were performed in Vivaspin 6 10 kDa molecular-weight cutoff sample concentrators (Vivascience). The protein stock for crystallization contained 19.0 mg ml^{-1} FP480 in 10 m*M* Tris–HCl pH 8.0, 100 m*M* NaCl, 2.5 m*M* EDTA. Crystals of FP480 were obtained by hanging-drop vapor diffusion from 1 µl protein solution mixed with 1 µl well solution [100 m*M* bis-tris pH 6.5, 25% PEG 3350, 200 m*M* $MgCl_2$ or 80 m*M* citric acid pH 3.5, 20%(*w*/*v*) PEG 3350] equilibrated against 500 µl of the same reservoir solution in one week at 293 K.

Table 1
Diffraction data statistics for the neutral pH form of FP480 processed in space group *I*422.

Values in parentheses are for the last resolution shell.

	Acidic pH form	Neutral pH form
Space group	*I*4	*I*422
Molecules per ASU	2	0.5
Unit-cell parameters (Å)	$a = b = 98.21$, $c = 108.06$	$a = b = 91.40$, $c = 53.53$
Resolution (Å)	30.0–2.0 (2.07–2.0)	30.0–2.4 (2.49–2.4)
Total reflections	146813	43378
Unique reflections	34954	4611
Completeness (%)	100.0 (100.0)	99.9 (100.0)
$I/\sigma(I)$	17.0 (2.7)	21.7 (3.0)
$R_{\rm merge}$	0.075 (0.534)	0.096 (0.695)
Multiplicity	4.2 (4.0)	9.4 (9.5)

The diffraction data for the neutral pH crystals were measured on the Advanced Photon Source GM/CA-CAT beamline ID23 and those for the acidic pH crystals were measured on SER-CAT beamline ID22 (Argonne National Laboratory). All diffraction images were processed with *HKL*-2000 (Otwinowski & Minor, 1997). The statistics of the diffraction data processing for both acidic and neutral pH FP480 are shown in Table 1.

Both structures of FP480 were solved by molecular replacement with *MOLREP* (Vagin & Teplyakov, 1997) from the *CCP*4 suite (Collaborative Computational Project, Number 4, 1994). Refinement was performed with *REFMAC*5 (Murshudov *et al.*, 1997), *PHENIX* (Adams *et al.*, 2002) and *SHELXL* (Sheldrick, 2008). Real-space model corrections were performed with *Coot* (Emsley & Cowtan, 2004). Structure quality was validated with *PROCHECK* (Laskowski *et al.*, 1993) and *Coot*. The coordinates were deposited in the Protein Data Bank and assigned accession codes 3h1o for the acidic form and 3h1r for the neutral crystal form.

3. Results and discussion

Both crystal types appeared to be single and well shaped and displayed a tetragonal *I*-centered lattice, but the low pH version had approximately twice the volume of the neutral pH form (Table 1). Reflections of the form (0, 0, 2*n*) were observed, precluding the presence of 4_1 or 4_3 screw axes. The structure of the low pH crystals of FP480 was easily solved and refined in space group *I*4 to an *R* factor of 0.178 and an $R_{\rm free}$ of 0.222. The detailed structure and function will be described elsewhere and will only be compared with the other (neutral

pH) form at the level of crystal packing. All references to the FP480 structure in the following sections relate to the neutral pH small unit-cell form of FP480 unless specified otherwise.

While the images obtained from the acidic pH FP480 crystals looked typical of a well ordered specimen, the diffraction patterns from the neutral pH crystals contained very faint and diffuse reflections between the principal well defined Bragg reflections (Fig. 1). These additional reflections were positioned in the a^*,b^* layers between the well shaped reflections and their streaks were elongated in the a^*,b^* plane. The sharp reflections and the streaked reflections could be indexed together on a primitive lattice with the c cell dimension doubled. Under such an indexing, reflections with $2h + 2k + l = 4n$ were well shaped while those with $2h + 2k + l = 2n + 1$ were weak and diffuse; the rest, with $2h + 2k + l = 4n + 2$, did not exist. Reflections from the first six diffraction images were processed in this larger primitive lattice assuming very elongated integration peak profiles to accommodate most of the streaked reflection shapes. The statistics of the measured intensities are shown in Table 2. The intensities of the diffuse reflections are approximately 50 times weaker than the intensities of the well shaped reflections, with an average $I/\sigma(I)$ of 0.4, which is below the level of a meaningful signal. These diffuse reflections were therefore neglected and the unit

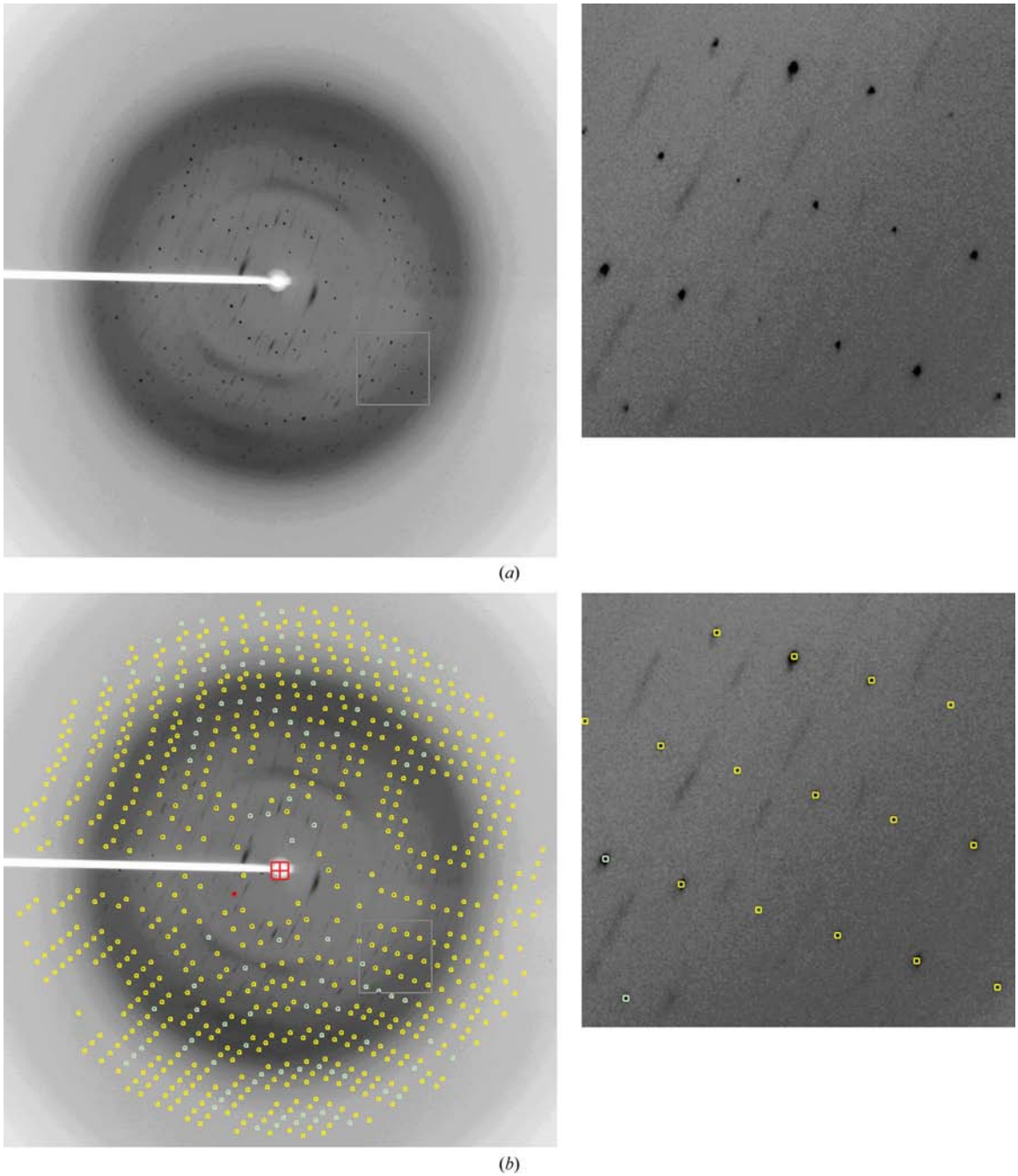

Figure 1
The diffraction pattern of FP480 crystals obtained at neutral pH. (*a*) Raw image; (*b*) the same image indexed with *HKL*-2000. The enlarged section of the frame shows the lines of diffuse reflections alternating with well shaped diffraction spots.

Table 2
Intensity statistics of reflections from the first six images of the neutral pH FP480 crystal indexed in the *P*422 cell with $a = b = 91.4$, $c = 107.0$ Å.

Type of reflection	$\langle I \rangle$	$\langle \sigma \rangle$	$\langle I/\sigma(I) \rangle$	No. of reflections
Well shaped, $2h + 2k + l = 4n$	587.6	27.8	14.2	671
Diffuse, $2h + 2k + l = 2n + 1$	10.0	41.5	0.4	1373
Non-existent, $2h + 2k + l = 4n + 2$	−1.1	27.9	−0.04	639

cell and data presented in Table 1 were used in all subsequent analyses.

Diffraction data from crystals of the neutral form merged satisfactorily in *I*4 and *I*422 symmetries, with an $R_{\rm merge}$ of 0.094 and 0.096, respectively. However, the volume of the cell could not accommodate even one monomer of FP480 with a molecular weight of 27 722 Da in the asymmetric unit of the *I*422 space group, which would have a $V_{\rm M}$ value of 1.01 Å^3 Da^{-1}. Therefore, there can be only four monomers of FP480 in this unit cell, with a $V_{\rm M}$ value of 2.02 Å^3 Da^{-1}. This behavior could be explained by the occurrence of merohedral twinning, which is theoretically possible in the *I*4 space group. However, the intensity statistics (Table 3) showed no characteristics typical of merohedral twinning, with a Wilson ratio $\langle I^2 \rangle / \langle I \rangle^2$ of 2.079, a nearly perfect shape of the $N(Z)$ plot (Fig. 2) and an L ratio of 0.509 (Padilla & Yeates, 2003). Since the data merge well in *I*422 symmetry, twinning criteria based on the comparison of intensities within pairs of potentially twin-related reflections, as in the *H*-test (Yeates, 1997) or the Britton test (Fisher & Sweet, 1980), are not applicable since these intensities are indeed equal. Taking this into account, we concluded that these crystals suffered from another pathology, namely the order–disorder (OD) phenomenon. The known cases of OD structures (alternatively referred to as structures with lattice-translocation defects) involve parallel translations between consecutive layers of molecules in the crystal, a phenomenon that manifests itself by the presence of significant off-origin peaks in the native Patterson map. However, for neutral pH FP480 the highest off-origin peaks in the native Patterson map are at the level of 4% of the origin peak or 4.5 standard deviations above the mean density. This excludes the presence of translational pseudosymmetry in the case presented here.

In its crystalline state, FP480 occurs as a tetramer of four monomers with 222 symmetry, an arrangement typical of the majority of classic fluorescent proteins. In the acidic form, the tetramers are placed at the special position on the 4_2 axis, which also includes one of the tetrameric twofold axes (Fig. 3*a*). The two remaining tetrameric twofold axes in this *I*4 structure are directed about 28° from the unit-cell axes *a* and *b*. The neighboring tetramers in the *a*,*b* layers are grouped in a chessboard-like fashion at 90° with respect to each other, as illustrated in Fig. 3(*a*). The upper layer of tetramers, at $z = \frac{1}{2}$, is related by the 4_2 symmetry operation, *i.e.* each tetramer is accompanied above (and below) by another one rotated by 90°.

The structure of the neutral form of FP480 was also easily solved by molecular replacement in either of the space groups *I*4 or *I*422. The results of both calculations were equivalent and delivered two possible orientations of the FP480 monomer, also forming tetramers. However, the solutions corresponded to two overlapping tetramers located at the special position 422 of the *I*422 cell, with the three tetrameric axes parallel to the crystallographic *c* direction and to two base diagonals of the tetragonal cell (Fig. 3*b*). The packing of these 'double' tetramers is different to that found in the previous crystal form. The tetramers located at the corners of the unit cell are interspersed by the tetramers located at the position $(\frac{1}{2}, \frac{1}{2}, \frac{1}{2})$, with half of the tetramer height above (and

Table 3
Intensity statistics of the neutral pH FP480 data.

	Observed	Theoretical	
	*I*422	Untwinned	50% twinned
Wilson ratios			
$\langle I^2 \rangle / \langle I \rangle^2$	2.079	2.0	1.5
Padilla & Yeates statistics†			
$\langle \lvert L \rvert \rangle$	0.509	0.5	0.375
$\langle L^2 \rangle$	0.342	0.333	0.2

† According to Padilla & Yeates (2003).

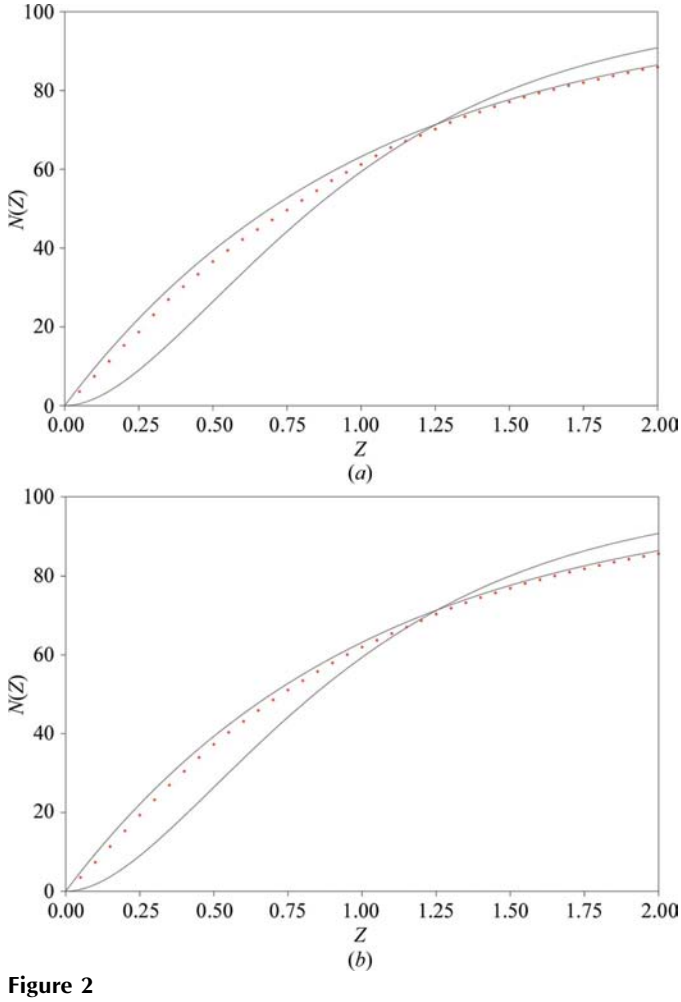

Figure 2
$N(Z)$ plots calculated for (*a*) the order–disorder FP480 crystal (neutral pH form) data and (*b*) the ordered FP480 crystal (acidic pH form) data. The exponential and sigmoidal black lines correspond to 'not twinned' and perfectly twinned theoretical cases, respectively. Red dots represent experimental statistics calculated from measured data.

half below) the previous tetramers. Obviously, a structure containing such overlapping molecules is not physically acceptable and should be treated as the result of a specific disorder. In a sense, this crystal structure has 'statistical' *I*422 symmetry (Fig. 3*b*), in which the tetrameric molecules in the individual unit cells are arranged according to lower symmetry (Figs. 3*c* and 3*d*). but the orientation of the molecules in different unit cells differs by 90°; these differently oriented molecules (or the whole groups of unit cells) are spread randomly throughout the crystal, giving rise to its OD organization. However, the presence of additional very weak and diffuse reflections in the diffraction pattern suggests that the randomness in the distribution of the alternatively oriented tetramers throughout the crystal is not perfect and that some degree of correlation exists.

In the classic OD phenomenon (Dornberger-Schiff, 1956), successive layers of molecules in the crystal are shifted in a particular direction by a positive or negative fractional displacement. Therefore, the perfect order within each layer is

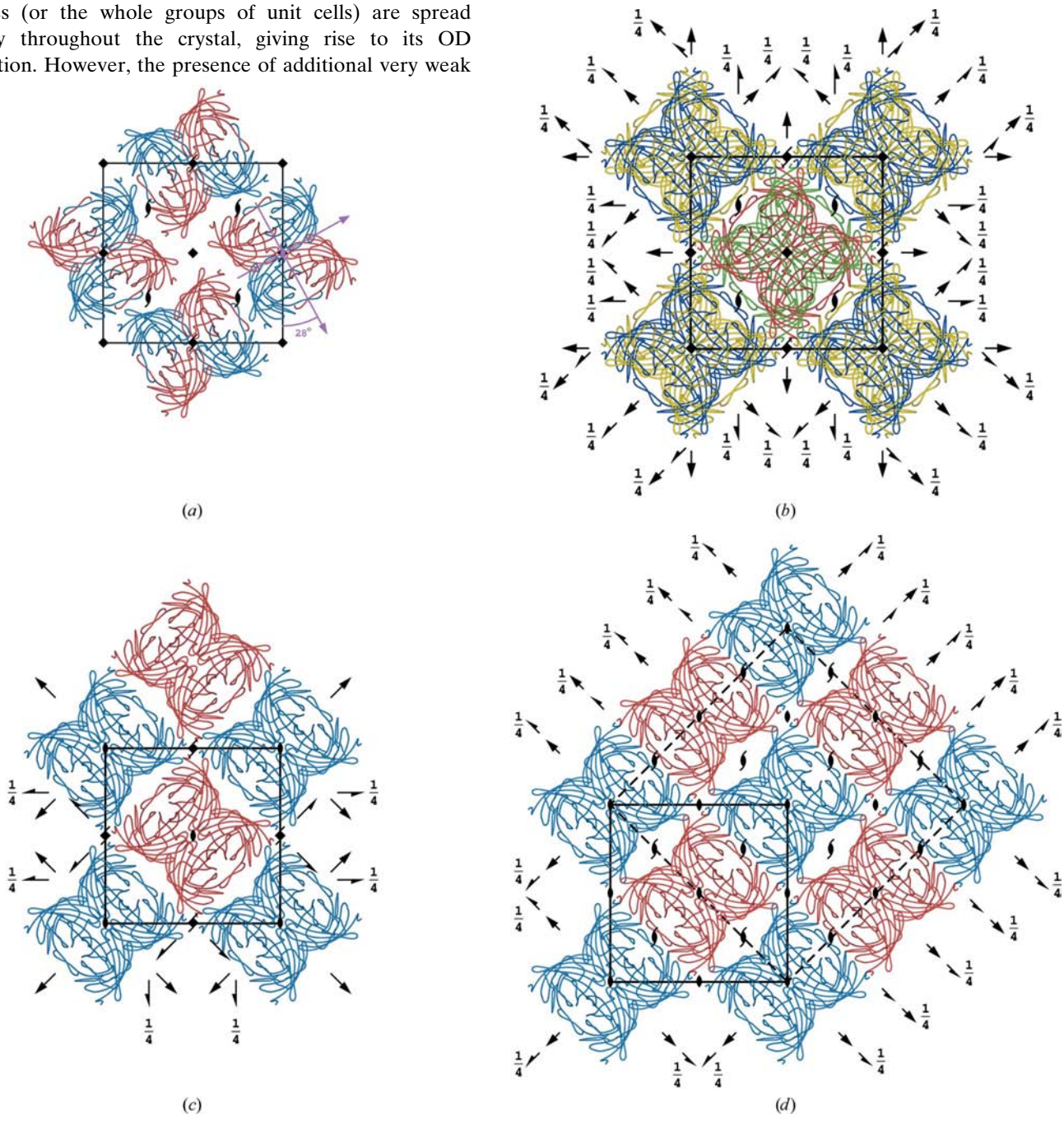

Figure 3
(*a*) Crystal packing of the acidic pH FP480 structure in space group *I*4, with two symmetry-independent molecules (related by noncrystallographic twofold axes) shown in blue and red. (*b*) Statistically averaged *I*422 order–disorder neutral pH FP480 structure, with a pair of blue and yellow tetramers overlapping at the corners of the unit cell and a pair of red and green tetramers overlapping at the cell center. (*c*) Theoretically possible packing of the neutral pH FP480 structure in $P4_22_12$, with blue tetramers at the unit-cell corners and red tetramers at the cell centers. (*d*) Another theoretically possible packing of the neutral pH FP480 structure, again with blue tetramers at the corners and red tetramers at the centers of the original nonstandard *I*212 cell or at the corresponding positions of the equivalent standard *F*222 cell marked with dashed black lines. The statistically averaged *I*422 structure represented in (*b*) results from rotating the (*c*) or (*d*) models by 90° and overlapping them on the initial models.

accompanied by disorder in the mutual relation of pairs of successive layers, hence the name of the phenomenon. Depending on the degree of randomness and the amount of the parallel offset in the packing of consecutive layers, the diffraction images of such crystals may contain certain reflections that are elongated or diffuse, as explained by Bragg & Howells (1954) and Cochran & Howells (1954).

The structure of the neutral pH FP480 can be explained in similar terms, in which the tetrameric molecules in the neighboring unit cells are not related by parallel displacements but are rotated by 90°, which is not a true crystallographic symmetry element of the structure. There are two possible symmetric arrangements of FP480 tetramers within individual unit cells which, after averaging according to the fourfold rotation, result in the 'statistical' *I*422 symmetry apparent in the diffraction data. Both possibilities are subgroups of the *I*422 space group where the tetramers occupy special positions with 222 symmetry. They are the two among the maximal subgroups of the *I*422 space group that have 222 special positions with two of the axes along diagonals between the *x* and *y* directions (*International Tables for Crystallography*, 2002). The first corresponds to the $P4_22_12$ space group (Fig. 3*c*), in which all tetramers at $z = 0$ are parallel and all tetramers at $z = \frac{1}{2}$ are perpendicular to the previous tetramers. Averaging such an arrangement using a 90° rotation produces the *I*422 arrangement of half-occupied and overlapping tetramers, as illustrated in Fig. 3(*b*).

The second possible ordered packing of tetramers corresponds to the *F*222 space group, in which all tetramers within the unit cell are parallel (Fig. 3*d*). Again, however, averaging by 90° rotation leads to an identical *I*422 arrangement as in the previous case. It is not possible to specify which of these two arrangements is really executed in the crystal. Since the diffraction data merge well in *I*422 symmetry and the additional diffuse reflections present in the diffraction patterns are very faint, it may be concluded that the average occurrence of tetramers rotated in two possible orientations is close to 50:50 and that their distribution is nearly random.

The neutral pH FP480 model containing two half-occupied and overlapping monomers in the asymmetric unit was refined in the *I*422 space group to an *R* factor of 0.228 and an $R_{\rm free}$ of 0.321, confirming the general correctness of the above analysis. Such an $R_{\rm free}$ value would be rather high for an ordinary well refined protein crystal structure. However, taking into account the scarcity of reflections in comparison with the number of refined parameters (which is increased twice by the presence of two half-occupied molecules) and the imperfect quality of the diffraction spots, the results show that our model is plausible, albeit not ideal. The results of the model refinement are included in Table 4. The $2F_{\rm obs} - F_{\rm calc}$ map covering intersecting fragments of β-strands from two alternatively oriented monomers is shown in Fig. 4(*a*) and the composite OMIT map around four different parts of a single monomer is presented in Fig. 4(*b*).

An alternative explanation (which is unlikely because of the nearly perfect intensity statistics) could be the presence of perfect merohedral twinning of the *F*222 structure. To explore this possibility, we performed *SHELXL* refinement of such a

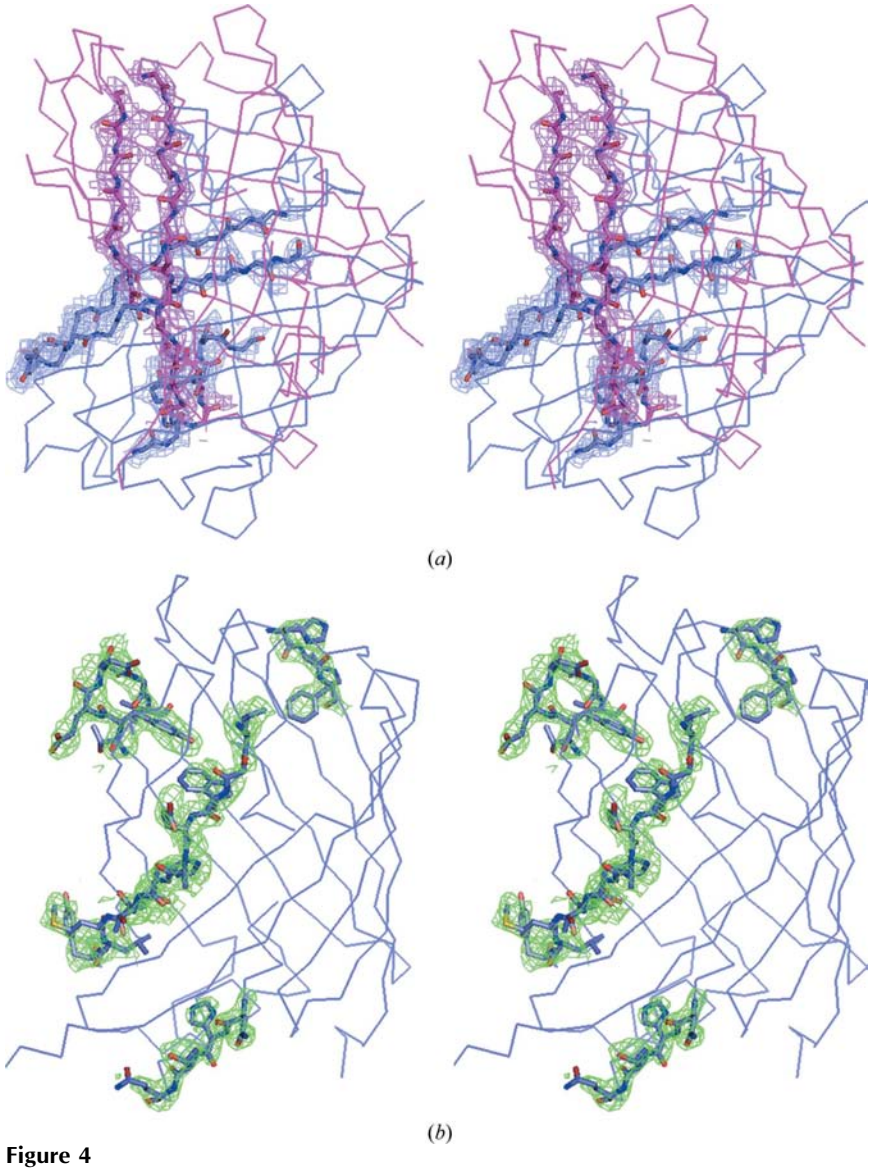

Figure 4
(*a*) Stereoview of a $2F_{\rm obs} - F_{\rm calc}$ map at the 1σ level around two β-strands selected from two overlapping monomers. For clarity, the overlapping monomers are shown as a C^{α} trace, but all main-chain atoms are shown in the regions surrounded by electron density. (*b*) Composite OMIT map at the 2σ level of four regions of a single monomer selected so that they do not overlap with the alternatively oriented molecule. The four OMIT maps were calculated separately and combined into one stereo illustration.

Table 4
Refinement statistics for acidic pH form and neutral pH form of the FP480 structure.

	Acidic pH form	Neutral pH form
Space group	*I*4	*I*422
Unit-cell parameters (Å)	$a = b = 98.2$, $c = 108.1$	$a = b = 91.4$, $c = 53.5$
Resolution (Å)	30–2.0	30–2.4
No. of reflections	37694	4161
R_{work}/R_{free}	0.178/0.222	0.228/0.321
No. of non-H atoms	3875	1797 (occupancy 0.5)
Geometry statistics		
Bonds (Å)	0.005	0.019
Angles (°)	0.72	2.11
Chirality (Å^3)	0.060	0.125
Planarity (Å)	0.003	0.011

model, assuming the nonstandard but equivalent *I*212 symmetry in the original *I*-centered lattice with appropriate 'BASF 0.5' and 'TWIN 1 0 0, 0 −1 0, 0 0 −1' commands. The obtained *R* value of 0.327 and the R_{free} of 0.467 suggest that such an interpretation can be excluded. Merohedral twinning is not possible in $P4_22_12$, since its point group is 422, which corresponds to the high symmetry of the lattice.

4. Conclusion

In the currently available literature, the meanings of order–disorder (OD) and lattice-translocation defects (LTD) are practically the same. The first term was introduced by Dornberger-Schiff (1956) and the second by Wang, Kamtekar *et al.* (2005). Both of these terms have been used to describe crystal structures in which successive layers of molecules are shifted with respect to each other in one direction or its reverse in a more or less random fashion. In our work, we observe another type of defect based on rotational disorder. This phenomenon falls into the category of OD structures, but it does not involve translational components. The present case is therefore best described as a rotational OD structure.

This study confirms that structural information can be successfully extracted not only from twinned crystals but also from rarer crystals suffering from order–disorder phenomena. While reports on twinned structures are becoming quite common owing to the notable evolution of crystallographic software, order–disorder structures still represent a challenge because no specialized algorithms exist to handle such cases automatically. The results described in this paper may be useful for program developers to extend the capabilities of crystallographic software. The diffraction images of FP480 crystals are available on request from SVP (svp@ncifcrf.gov) or ZD (dauter@anl.gov).

This work was supported in part by Federal funds from the National Cancer Institute, National Institutes of Health (NIH; contract No. HHSN261200800001E), the Intramural Research Program of the NIH, National Cancer Institute, Center for Cancer Research and by a grant from the NIH (GM073913) to VVV. The content of this publication does not necessarily reflect the views or policies of the Department of Health and Human Services, nor does the mention of trade names, commercial products or organizations imply endorsement by the US Government. Diffraction data were collected on the SER-CAT ID22 and GM-CA/CAT 23ID beamlines at the Advanced Photon Source, Argonne National Laboratory. Use of the Advanced Photon Source was supported by the US Department of Energy, Office of Science, Office of Basic Energy Sciences under Contract No. W-31-109-Eng-38.

References

Adams, P. D., Grosse-Kunstleve, R. W., Hung, L.-W., Ioerger, T. R., McCoy, A. J., Moriarty, N. W., Read, R. J., Sacchettini, J. C., Sauter, N. K. & Terwilliger, T. C. (2002). *Acta Cryst.* D**58**, 1948–1954.
Berman, H. M., Westbrook, J., Feng, Z., Gilliland, G., Bhat, T. N., Weissig, H., Shindyalov, I. N. & Bourne, P. E. (2000). *Nucleic Acids Res.* **28**, 235–242.
Bragg, W. L. & Howells, E. R. (1954). *Acta Cryst.* **7**, 409–411.
Brünger, A. T., Adams, P. D., Clore, G. M., DeLano, W. L., Gros, P., Grosse-Kunstleve, R. W., Jiang, J.-S., Kuszewski, J., Nilges, M., Pannu, N. S., Read, R. J., Rice, L. M., Simonson, T. & Warren, G. L. (1998). *Acta Cryst.* D**54**, 905–921.
Cochran, W. & Howells, E. R. (1954). *Acta Cryst.* **7**, 412–415.
Collaborative Computational Project, Number 4 (1994). *Acta Cryst.* D**50**, 760–763.
Dauter, Z., Botos, I., LaRonde-LeBlanc, N. & Wlodawer, A. (2005). *Acta Cryst.* D**61**, 967–975.
Dhillon, A. K., Stanfield, R. L., Gorny, M. K., Williams, C., Zolla-Pazner, S. & Wilson, I. A. (2008). *Acta Cryst.* D**64**, 792–802.
Dornberger-Schiff, K. (1956). *Acta Cryst.* **9**, 593–601.
Dornberger-Schiff, K. & Grell-Niemann, H. (1961). *Acta Cryst.* **14**, 167–177.
Emsley, P. & Cowtan, K. (2004). *Acta Cryst.* D**60**, 2126–2132.
Fisher, R. G. & Sweet, R. M. (1980). *Acta Cryst.* A**36**, 755–760.
Glauser, S. & Rossmann, M. G. (1966). *Acta Cryst.* **21**, 175–177.
Hwang, W. C., Lin, Y., Santelli, E., Sui, J., Jaroszewski, L., Stec, B., Farzan, M., Marasco, W. A. & Liddington, R. C. (2006). *J. Biol. Chem.* **281**, 34610–34616.
International Tables for Crystallography (2002). Vol. *A*, edited by T. Hahn, p. 369. Dordrecht: Kluwer Academic Publishers.
Laskowski, R. A., MacArthur, M. W., Moss, D. S. & Thornton, J. M. (1993). *J. Appl. Cryst.* **26**, 283–291.
Lebedev, A. A., Vagin, A. A. & Murshudov, G. N. (2006). *Acta Cryst.* D**62**, 83–95.
Lietzke, S. E., Carperos, V. E. & Kundrot, C. E. (1996). *Acta Cryst.* D**52**, 687–692.
Murshudov, G. N., Vagin, A. A. & Dodson, E. J. (1997). *Acta Cryst.* D**53**, 240–255.
Otwinowski, Z. & Minor, W. (1997). *Methods Enzymol.* **276**, 307–326.
Padilla, J. E. & Yeates, T. O. (2003). *Acta Cryst.* D**59**, 1124–1130.
Pickersgill, R. W. (1987). *Acta Cryst.* A**43**, 502–506.
Rye, C. A., Isupov, M. N., Lebedev, A. A. & Littlechild, J. A. (2007). *Acta Cryst.* D**63**, 926–930.
Schulze-Gahmen, U., Rini, J. M. & Wilson, I. A. (1993). *J. Mol. Biol.* **234**, 1098–1118.
Sheldrick, G. M. (2008). *Acta Cryst.* A**64**, 112–122.
Tanaka, S., Kerfeld, C. A., Sawaya, M. R., Cai, F., Heinhorst, S., Cannon, G. C. & Yeates, T. O. (2008). *Science*, **319**, 1083–1086.
Trame, C. B. & McKay, D. B. (2001). *Acta Cryst.* D**57**, 1079–1090.
Vagin, A. & Teplyakov, A. (1997). *J. Appl. Cryst.* **30**, 1022–1025.
Wang, J., Kamtekar, S., Berman, A. J. & Steitz, T. A. (2005). *Acta Cryst.* D**61**, 67–74.
Wang, J., Rho, S.-H., Park, H. H. & Eom, S. H. (2005). *Acta Cryst.* D**61**, 932–941.
Yeates, T. O. (1997). *Methods Enzymol.* **276**, 344–358.
Zhu, X., Xu, X. & Wilson, I. A. (2008). *Acta Cryst.* D**64**, 843–850.